Quantitative LEED *I-V* and *ab initio* study of the Si(111)-3×2-Sm surface structure and the missing half-order spots in the 3×1 diffraction pattern

C. Eames, M. I. J. Probert, and S. P. Tear*
Department of Physics, University of York, York YO10 5DD, United Kingdom
(Received 19 November 2006; revised manuscript received 21 February 2007; published 15 May 2007)

We have used low-energy electron diffraction (LEED) *I-V* analysis and *ab initio* calculations to quantitatively determine the honeycomb chain model structure for the Si(111)-3×2-Sm surface. This structure and a similar 3×1 recontruction have been observed for many alkali-earth and rare-earth metals on the Si(111) surface. Our *ab initio* calculations show that there are two almost degenerate sites for the Sm atom in the unit cell, and the LEED *I-V* analysis reveals that an admixture of the two in a ratio that slightly favors the site with the lower energy is the best match to experiment. We show that the *I-V* curves are insensitive to the presence of the Sm atom and that this results in a very low intensity for the half-order spots, which might explain the appearance of a 3×1 LEED pattern produced by all of the structures with a 3×2 unit cell.

DOI: 10.1103/PhysRevB.75.205420 PACS number(s): 61.46.−w, 61.14.Hg, 68.43.Bc

I. INTRODUCTION

The prospect of creating an ordered one-dimensional system has led to the extensive study of chain structures grown on surfaces. The alkali metals (AMs) form such a chain structure as part of a 3×1 reconstruction on the Si(111) surface with an AM coverage of 1/3 ML (Refs. 1 and 2, and references therein). At a coverage of 1/6 ML, the alkali-earth metals (AEMs) and the rare-earth metals (REMs) form a 3×2 reconstruction (Refs. 3–6, and references therein). There is a wealth of experimental evidence from scanning tunneling microscopy (STM), low-energy electron diffraction (LEED), and spectroscopic techniques to suggest that in these 3× structures, there is a common structure for the reconstructed silicon (Refs. 3–11, and references therein). The honeycomb chain channel (HCC) model is now regarded by many as the most plausible of the candidate structures.[12–14] In the HCC model, there are parallel ordered one-dimensional lines of metal atoms sited in a silicon-free channel. These are separated by almost flat honeycomb layers of silicon.

The 3×1 system has been studied using LEED *I-V* analysis with Ag, Li, and Na as the deposited metal atoms.[11] Similar *I-V* curves were obtained in each case, and the authors conclude that a common reconstruction of silicon atoms is responsible for the LEED *I-V* curves, which are insensitive to the presence of the metal atom. However, the authors did not attempt a structural fit. The LEED pattern for the 3×2 surfaces exhibits odd behavior in that it indicates a 3×1 periodicity. Many workers have suggested that disorder in the position of the metal atom is the cause. A Fourier analysis of a random tesselation of a large sample of registry shifted 3×2 unit cells has been carried out by Schäfer *et al.*[15] They show that this simulation of long-range disorder in the position of the metal atom does produce a 3×1 periodicity in reciprocal space. Alternatively, Over *et al.*[16] have suggested that the substrate and silicon adatoms could be acting as the dominant scattering unit, with the metal atoms sitting in "open sites."

STM investigations of the 3×2 and 3×1 systems have not provided much evidence of long-range disorder in the location of the metal atom apart from registry shifts introduced by a coexisting $c(6\times2)$ phase. Of particular relevance to this work is the study of the Si(111)-3×2-Sm system using STM and an *ab initio* calculation, carried out by Palmino *et al.*[5] They have used the bias voltage dependence of the STM images of the surface to isolate the features associated with the honeycomb chain and the samarium atom, and a separate comparison of these with simulated STM images obtained from the *ab initio* calculation shows that the HCC structure is in good lateral qualitative agreement with experiment.

In this study, we have used LEED *I-V* analysis and several *ab initio* calculations to quantitatively investigate the 3×2 reconstruction of the Si(111)-3×2-Sm surface. We show that the HCC structure gives good agreement with experiment. We consider two HCC unit cells in which the samarium atom is located in the T4 site or the H3 site. Palmino *et al.*[5] have found the energy difference of these two configurations to be 0.07 eV/Sm. We have calculated the atomic positions and the energies of these two reconstructions and obtained LEED *I-V* curves for this system, and we show that a linear combination of the two HCC structures is the optimum match to experiment, with a ratio that slightly favors the structure with the lower energy of the two.

We have also used LEED *I-V* analysis to investigate the missing half-order spots for the 3×2 unit cell. We show using calculated *I-V* curves that for an individual unit cell, the intensity of the half-order spots is significantly lower than that of the spots that are visible in the experiments. We also show that the calculated *I-V* curves do not differ significantly if the samarium atom is not present. We offer this as evidence that disorder over multiple unit cells is not needed to explain the discrepancy between LEED and STM for the 3×2 systems, and we suggest that the order in the one-dimensional chain may persist over large length scales.

II. EXPERIMENT

A dedicated LEED chamber of in-house design[17] operating at a typical UHV base pressure of $\sim10^{-10}$ mbar was used

 ©2007 The American Physical Society

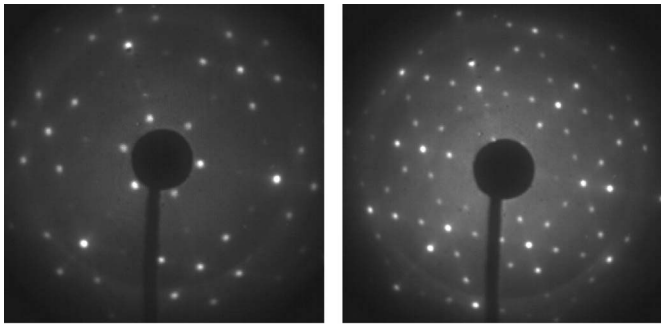

(a) (b)

FIG. 1. Experimental 3×1 LEED spot pattern for the Si(111)-3×2-Sm surface shown at (a) 40 eV and (b) 80 eV.

to carry out our experiments. The silicon substrate was cleaned by flashing to ≈1200 °C using an electron-beam heater and then the sample was slowly cooled through the ≈900–700 °C region over a period of 15 min. A sharp 7×7 LEED pattern resulted, confirming that a clean Si(111)-7×7 surface had been made. Temperatures were monitored using an infrared pyrometer.

In the literature, other workers[5,9,18] have formed the Si(111)-3×2-Sm structure by depositing 1/6 ML onto a sample held at a temperature of 400–850 °C, followed by annealing at this temperature for 20 min. In this work, the sample was prepared by depositing 1 ML of Sm from a quartz crystal calibrated evaporation source onto the clean Si(111)-7×7 surface, which was not at elevated temperature. This was followed by a hot anneal at ≈700 °C for 15 min. A sharp 3×1 LEED pattern was observed and images of this are shown in Fig. 1. Other workers have observed some streaking in the 3×1 LEED pattern that is indicative of one-dimensional disorder. We have not observed such streaking in our diffraction patterns, and we attribute this to our preparation procedure. There is some variability in the annealing temperature that can be used, and temperatures in the range ≈700–900 °C all gave a sharp diffraction pattern. It is at around 1000 °C that the pattern begins to degrade as the samarium desorbs.

Images of the diffraction pattern were acquired over a 40–250 eV range of primary electron energies in steps of 2 eV using a charge coupled device camera and stored on an instrument dedicated computer. For each spot in the LEED pattern, the variation in its intensity with primary electron energy was recorded, which resulted in a set of 42 *I-V* curves.

Degenerate beams were averaged together to reduce the signal-to-noise ratio and also to reduce any small errors that may have occurred in setting up normal beam incidence. Figure 2 defines the spot labeling system and the degenerate beams. The experiment was repeated several times and the *I-V* curves obtained during different experiments were compared using the Pendry *R* factor.[19] The *R* factor for *I-V* curves obtained on different days was typically 0.1 or less, which indicates that the surface is repeatedly preparable. To further reduce noise, the *I-V* curves from separate experiments were averaged together and a three point smooth was applied.

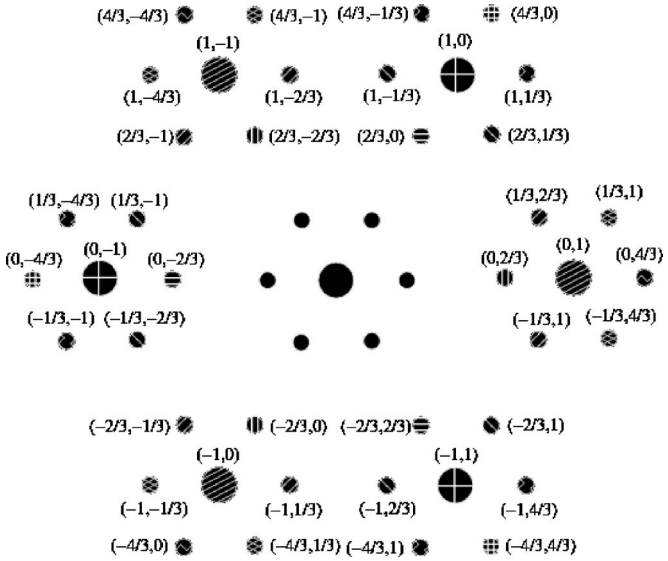

FIG. 2. Labeled spots in the 3×1 LEED pattern produced by the Si(111)-3×2-Sm surface as it appears at 40 eV. The degeneracies of the spots are indicated by the pattern used to fill each spot.

This set of 13 averaged *I-V* curves was used to fingerprint the surface structure and allow comparison with the *I-V* curves calculated for the various trial structures.

III. *AB INITIO* CALCULATIONS

Ab initio calculations were performed using the CASTEP code.[20] The code was run on 30 processors in a parallel computing environment at the HPCx High Performance Computing facility located at the CCLRC Daresbury Laboratory in the UK. We have geometry optimized two different unit cells for the HCC structure (see Fig. 5 for details). In the first unit cell, the samarium atom is located in the T4 site with respect to the first bulklike silicon layer, and in the other unit cell, the samarium atom is situated in an H3 site. We will refer to the two structures as "T4" and "H3." The initial atomic positions were those that were obtained in the *ab initio* study by Palmino *et al.*,[5] and these were very kindly provided by Palmino.

Before proceeding the input parameters in the calculation were carefully checked (see Ref. 21 for a discussion of its importance). Figure 3 shows how the calculated energy varies with the number of plane waves included in the calculation as the cutoff energy is raised for three increasingly dense Monkhorst-Pack[22] reciprocal space sampling grids.

A cutoff energy of 380 eV yields a total energy that is unambiguously in the variational minimum and will allow accurate calculation of the energy and the forces within the system. We have used the sampling grid with three *k* points in reciprocal space since an increase to six *k* points does not significantly change the energy. The Perdew-Burke-Ernzerhof[23] generalized gradient approximation was used to represent exchange and correlation effects.

The vacuum gap that was used to prevent interaction between the top surface in one supercell and the bottom surface in the supercell above was 9 Å thick, and this has been optimized during the course of other *ab initio* studies of rare-

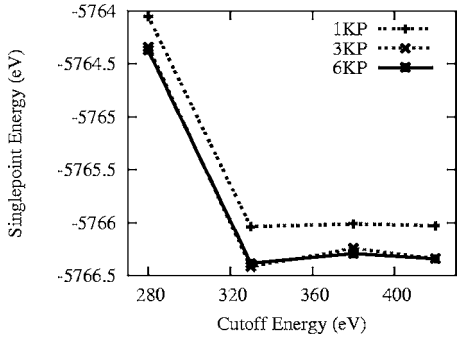

FIG. 3. Variation of the single point energy, which is the calculated energy for a given configuration of the atomic positions, with the cutoff energy and with the number of k points at which the wave function is sampled in reciprocal space.

earth silicides that we have done. We have included two bulklike silicon layers below the top layer that contains the samarium atom and the honeycomb chain structure. To prevent interactions through the supercell between uncompensated charge in the top and bottom layers and to fully replicate the transition to the bulk silicon crystal, we have hydrogen passivated the deepest bulklike silicon layer and fixed the coordinates of these atoms so that they are not free to move from their bulk positions. We have repeated the geometry optimization of the unit cells without passivation and positional constraints, and the final positions of the silicon atoms in this bottom layer are not drastically altered and

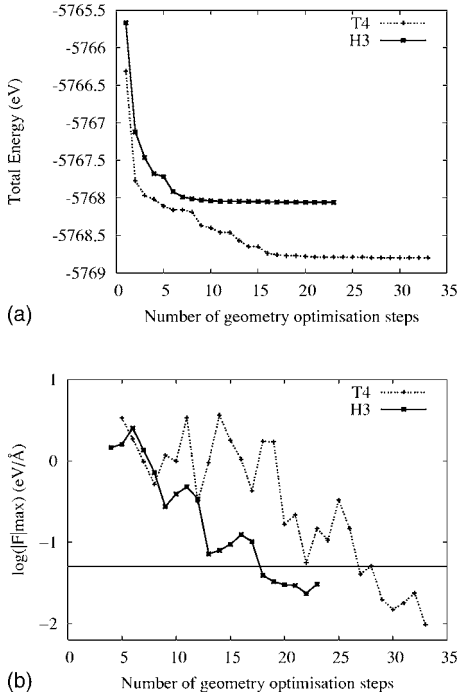

FIG. 4. Convergence of the total energy (top) and logarithmic convergence of the forces (bottom) during the geometry optimization of the T4 and H3 structures. The horizontal line indicates the force convergence tolerance of 5×10^{-2} eV/Å. The T4 structure has a lower energy than the H3 structure and the maximum force on any atom is lower.

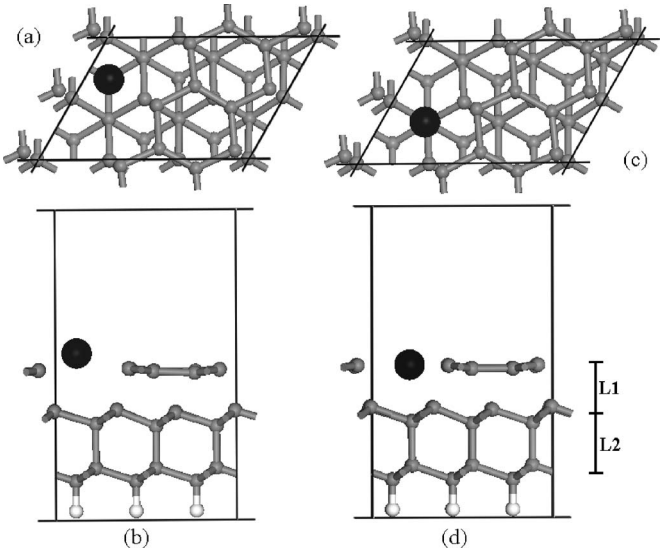

FIG. 5. Optimized structures for the HCC model showing the H3 model from above (a) and in side view (b), and the T4 model from above (c) and in side view (d). Silicon atoms here are gray, the samarium atom is black, and the hydrogen atoms are white. The first and second interlayer spacings are labeled L1 and L2, respectively.

the total energy does not significantly change as a result, which suggests that using so few bulklike layers is reasonable. We, nevertheless, kept the hydrogen passivation in place since it reduces the computational cost of the electronic structure calculation by the quenching of dangling bonds on the underside of the supercell.

The structures were allowed to relax until the forces were below the predefined tolerance of 5×10^{-2}eV/Å. Figure 4 shows the convergence of the total energy and the maximum force on any atom as the geometry optimization proceeds for the two structures.

The T4 structure is 0.7 eV (0.01%) lower in energy than the H3 structure and the maximum force in the system is slightly lower. This energy difference cannot be quantitatively compared with the value of 0.07 eV/Sm that was obtained in Ref. 5 since this is an atomically resolved energy difference, whereas the value presented here compares the total energies of the two supercells with contributions from all of the atoms within. Also, one cannot compare the basis set parameters used in this work with those presented in Ref. 5 since the two calculations used different types of pseudopotentials and a different *ab initio* code.

The final optimized structures are shown in Fig. 5. The interlayer spacings (ignoring the samarium atom for now) in both structures here are almost identical. The major difference between this calculated structure and that in Ref. 5 is in the interlayer spacings. In this study, the spacing between the top layer and the first bulklike layer (L1 in Fig. 5) is approximately 8% greater than that in Ref. 5 and the spacing between the first bulklike layer and the second bulklike layer (L2 in Fig. 5) is about 4% greater. There are also some minor differences in the position of the silicon atoms in the honeycomb chain.

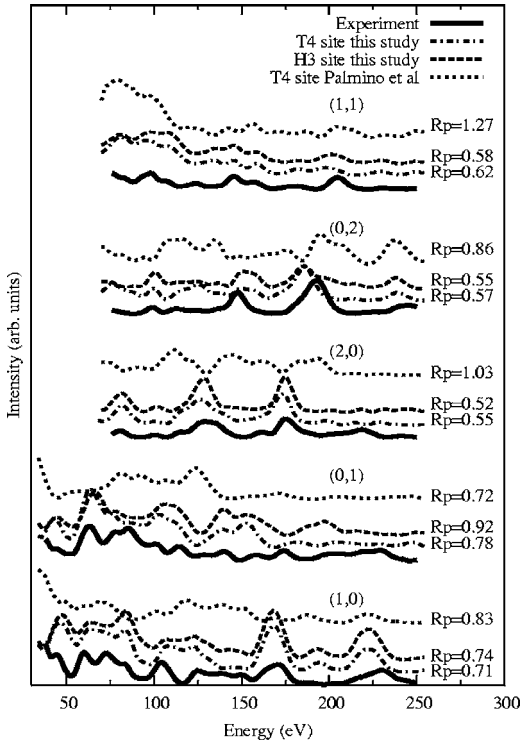

FIG. 6. A comparison of the *I-V* curves calculated for the integer spots for the structures suggested by the *ab initio* calculations in this study and elsewhere with those obtained experimentally. The *R* factor beside each curve indicates the level of agreement with experiment.

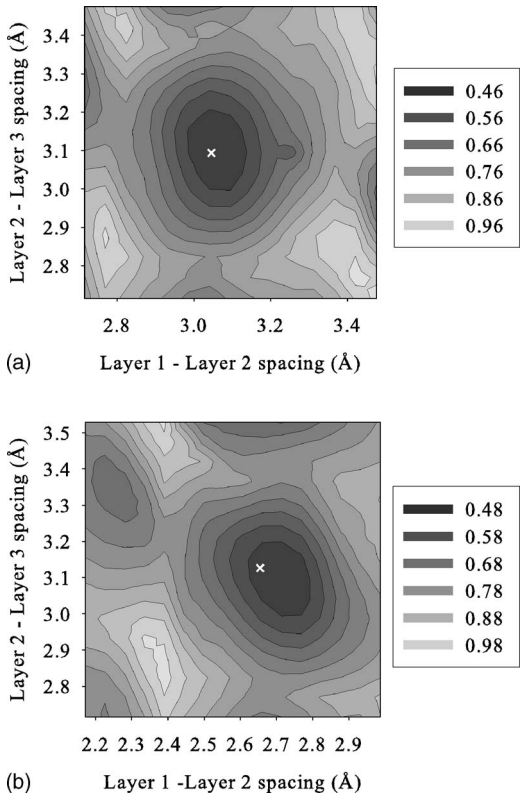

FIG. 7. Pendry *R*-factor landscape for a range of values of the interlayer spacings in the (a) H3 and (b) T4 structures for the fractional spots. The step size was 0.05 Å. The cross indicates the *ab initio* energy minimum.

IV. COMPARISON OF EXPERIMENT AND THEORY

Figure 6 shows *I-V* curves calculated using the CAVLEED code[24] for the three candidate *ab initio* structures. The curves shown are only the integer spots in the LEED pattern and they were calculated using the bulk Debye temperatures (that is, 645 K for silicon and 169 K for samarium) to represent the lattice vibrations of each layer. The structures obtained from the two *ab initio* calculations in this study are a consistently better match to experiment than those in Ref. 5. This suggests that the interlayer spacings obtained in this study, to which LEED is very sensitive, are closer to those present in the real surface. Also, note that the *I-V* curves of the T4 and H3 structures from this study are very similar and we cannot discard either structure.

We can divide the spots in the LEED pattern into two groups. The integer spots [(1,0), (2,0), (1,1), etc.] contain a large contribution from the bulk and are sensitive to the top few layers. The fractional spots [(2/3,0), (1/3,1), etc.] are extremely sensitive to the top layer reconstruction and only mildy sensitive to deeper layers through multiple scattering.

The poor Pendry *R* factors (that is >0.7 in this context, where enhanced vibrations have not been applied) for some of the integer spots in Fig. 6 indicate that further structural optimization is needed. It is apparent that for some curves the right peaks are present, but that their energy is slightly wrong [see the (0,2) and (2,0) spots in Fig. 6, for example]. The fractional spots have much better *R* factors (see Fig. 7), which indicates that the structure of the top layer is in good agreement with experiment. The natural way to proceed is to vary the interlayer spacings to attempt an improvement in the match with experiment, particularly for the integer spots. This is attempted in the next section.

V. LEED *I-V* STRUCTURAL OPTIMIZATION

The calculation of the *I-V* curves was repeated using various values for the interlayer spacings and the *R* factors were determined. An initial coarse search was carried out over a wide range of values for the spacings and with a large step size. Figure 7 shows the *R* factor landscape obtained in this manner for the fractional spots. There is a clear minimum in both cases. The samarium atom has been considered in determining the midpoint of the top layer, which is why the minima do not coincide; the samarium atom sits proud of the honeycomb layer in the H3 structure and it is much lower in the T4 structure. In the *ab initio* calculations in this study, the interlayer spacings were approximately 3.06 and 3.10 Å for the H3 structure and 2.65 and 3.14 Å for the T4 structure, which places the *ab initio* energy minimum (indicated by a cross in Fig. 7) very close to that of the CAVLEED *I-V R* factor minimum. Two independent techniques are thus suggesting very similar best-fit structures.

I-V curves were then obtained using a narrower range of interlayer spacings focused on the minima obtained in the coarse search. This fine search, using a step size of 0.01 Å,

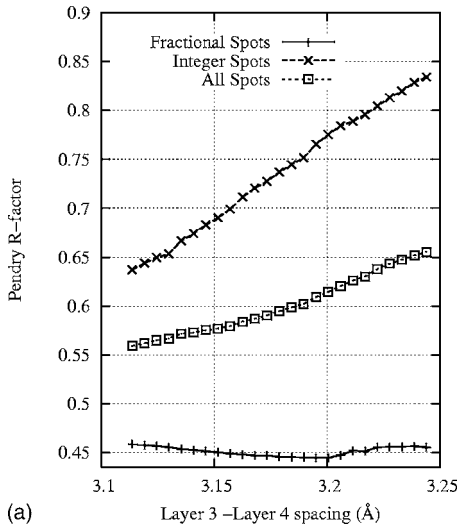

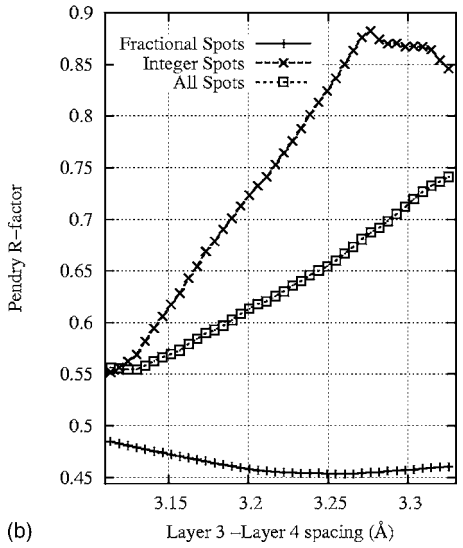

FIG. 8. Variation of the spacing between layers 3 and 4 in Si(111)-3×2-Sm for the H3 (a) and T4 (b) structures. The bulk value for this interlayer spacing is 3.14 Å.

improved the *R* factors by only around 0.01 in both cases, and even finer searches were not carried out.

There is another interlayer spacing deeper into the bulk that we might try to vary. Computational resources do not permit us to independently vary this spacing along with those between the top three layers. Figure 8 shows the variation of the Pendry *R* factor as the spacing between layers 3 and 4 is changed, with the first and second interlayer spacings fixed at their optimum value. We can see that there is a small improvement in the *R* factor for the fractional spots at the expense of a large worsening of the *R* factor for the integer spots, which are more sensitive to structure in the near bulk. We therefore reject any variation of this interlayer spacing and retain the bulk value. That there is no significant reconstruction deeper into the surface justifies the use of three layers in our *ab initio* calculation and means that in both the *ab initio* calculation and the Pendry *R* factor structure fit to the experimental data we have considered two interlayer spacings.

TABLE I. Variation of the Debye temperature for the samarium atom, silicon honeycomb layer, and first bulklike layer, and the effect on the Pendry *R* factors for the H3 structure. The naming scheme here is Sm, samarium atom; Si1, silicon honeycomb atoms; and Si2, first silicon bulklike layer. A Debye temperature of *B* indicates the bulk unoptimized value for that atomic species. Similar data are available for the T4 structure. Further enhancement of the vibrations of the samarium atom worsens the *R* factors.

Sm T_D	Si1 T_D	Si2 T_D	R_P^{frac}	R_P^{int}	R_P^{all}
B	B	B	0.49	0.72	0.63
$B/\sqrt{2}$	$B/3$	$B/2$	0.48	0.46	0.48
$B/2$	$B/3$	$B/2$	0.45	0.44	0.45

A. Optimization of the vibrations used in the LEED *I-V* calculation

The effect of thermal vibrations within the system has also been investigated. The Debye temperature T_D of the samarium atom, the silicon atoms in the honeycomb layer, and the silicon atoms in the first bulklike layer have each been independently reduced by a factor of $\sqrt{2}$, 2, and 3 respctively, from their bulk values. The effects of these enhanced vibrations for the two most effective combinations are shown in Table I alongside the *R* factors obtained with no enhanced vibrations.

The two schemes of enhanced vibrations both reduce the overall *R* factor by around 0.2, and this is mainly due to the improvement in the *R* factors of the integer spots.

B. Linear combination of the two candidate structures

The H3 and T4 structures have similar energies, similar structures (ignoring the position of the samarium atom), and similar LEED *I-V* curves. It is reasonable to suggest that both structures might coexist on the surface. A linear combination of the *I-V* curves produced by the H3 and T4 structures that individually best fit the experimental data is shown in Fig. 9 for the two regimes of enhanced vibration shown in Table I. The H3 and T4 structures are considered as being separated by a distance greater than the coherence length of the LEED beam. To simulate large and separate domains of the two structures in this way, the LEED spot intensities have been combined and not the amplitudes.

The vibrational regime with a Debye temperature for the samarium atom of 119 K ($B/\sqrt{2}$ in Table I) gives a lower *R* factor for the fractional order spots, but it gives a worse overall *R* factor. The vibrational regime with a Debye temperature for the samarium atom of 84 K ($B/2$ in Table I) gives a better overall *R* factor and the minima for both the fractional and integer spots coincide. The final ratio of H3 40:60 T4 is in favor of the structure that is lower in energy, which is what we would expect.

Table II contains a summary of the structures obtained from the *ab initio* calculations and from the CAVLEED LEED *I-V* structure fit. Two values are given for L1; the value in brackets ignores the Sm atom in determining the midpoint of the top layer. For the T4 structure, the Sm atom is almost

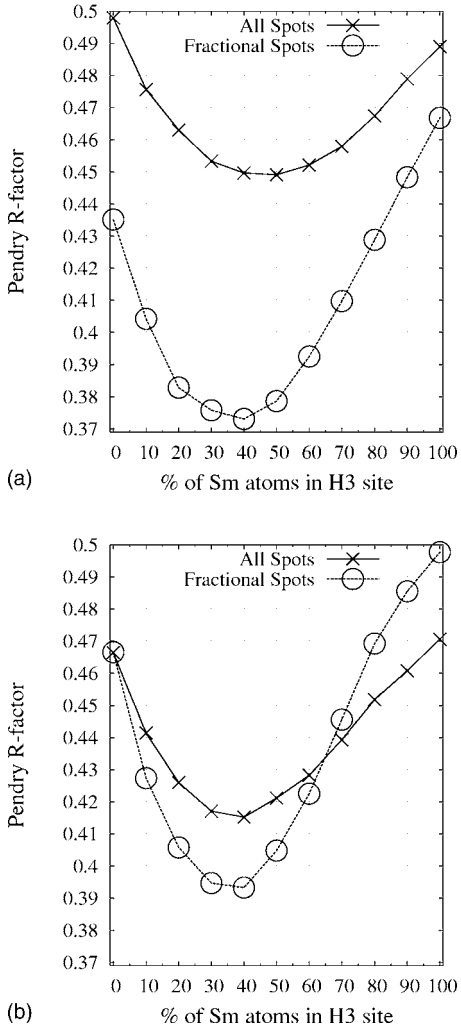

FIG. 9. Pendry R factors for a linear combination of the spot intensities of the H3 and T4 structures in various mixing ratios for two different vibrational regimes. In (a) the Debye temperature for the samarium atom is 119 K, and in (b), it is 84 K. In both cases, the Debye temperatures of the top silicon honeycomb layer, the first silicon bulklike layer, and the repeated bulk layer are 215, 323, and 645 K, respectively.

coplanar with the honeycomb layer, whereas for the H3 structure, the Sm atom sits proud of the surface and skews the value of L1. The value in brackets thus indicates the similarity of the spacings between the layers of silicon atoms in the two supercells. For each of the structures in this table, LEED I-V curves were calculated with optimized vibrations using a Debye temperature for the samarium atom of 84 K. These were then compared against experiment, and the Pendry R factors are included in Table II. The final optimized LEED I-V curves for the linear combination are compared with experiment for the integer spots in Fig. 10 and for the fractional spots in Fig. 11.

VI. LEED I-V INVESTIGATION OF THE MISSING HALF-ORDER SPOTS

The silicon honeycomb layer is almost mirror symmetric about a plane perpendicular to the $\times 2$ direction. It is the location of the samarium atom that breaks this mirror symmetry and renders a quasi 3×1 unit cell into a 3×2 unit cell. Figure 12 shows calculated I-V curves for the H3 structure for the fractional and integer spots compared with those for the same structure with the samarium atom removed. The bulk Debye temperatures were used throughout to minimize the influence of vibrations. It is readily apparent that the I-V curves are insensitive to the presence of the samarium atom.

This is not to say that the samarium atom is not a strong scatterer. It would appear that the silicon honeycomb layer as a scattering unit of eight atoms contributes much more to the I-V curves than the single samarium atom. A similar effect was observed in the LEED I-V structural analysis of Ag- and Li-induced Si(111)-$(\sqrt{3}\times\sqrt{3})R°$ by Over *et al.*[25] and was suggested as a cause for the 3×1 and/or 3×2 discrepancy in Ref. 16.

TABLE II. Pendry R factors for the fractional spots (R_P^{frac}), integer spots (R_P^{int}), and for all spots (R_P^{all}) for the various optimized structures in this work. All of the calculated I-V curves used optimized vibrations. The interlayer spacings are shown in columns five and six. The value of L1 in brackets ignores the Sm atom in the determination of the midpoint of the top layer and indicates the similarity of the structure of the silicon atoms in the two supercells.

Structure	R_P^{frac}	R_P^{int}	R_P^{all}	L1 (Å)	L2 (Å)
T4 (Ref. 5)	0.87	0.88	0.92	2.42 (2.52)	3.02
T4 CASTEP	0.44	0.46	0.46	2.65 (2.67)	3.14
H3 CASTEP	0.47	0.43	0.45	3.06 (2.62)	3.10
T4 CAVLEED	0.48	0.41	0.46	2.74 (2.73)	3.10
H3 CAVLEED	0.45	0.44	0.45	3.06 (2.64)	3.11
Combination	0.39	0.42	0.41	2.87 (2.69)	3.10

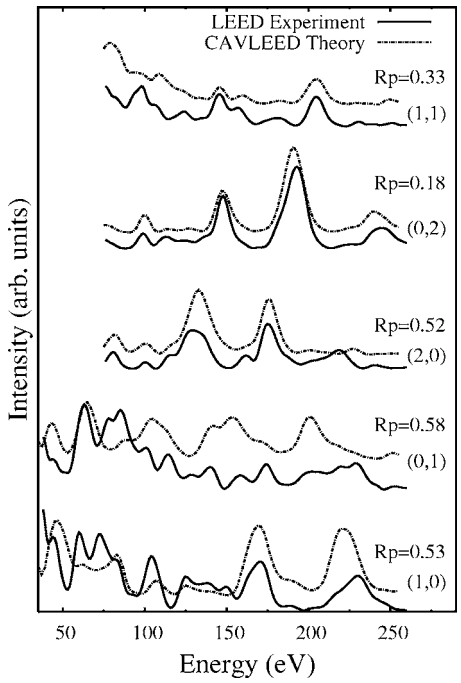

FIG. 10. Best-fit I-V curves for the integer LEED spots of the Si(111)-3×2-Sm structure.

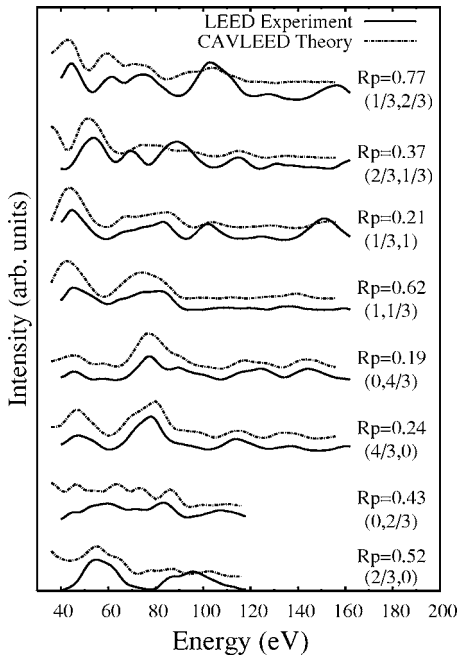

FIG. 11. Best-fit *I-V* curves for the fractional LEED spots of the Si(111)-3×2-Sm structure.

If this is the case, then the half-order spots that are apparently missing when the experimental 3×1 LEED pattern is inspected visually should produce calculated *I-V* curves whose intensity is very much less than that of the spots that are visible during experiment. The silicon honeycomb layer is not perfectly symmetrical about the mirror plane perpendicular to the ×2 direction and this should contribute to the half-order spot intensities. Figure 13 shows the *I-V* curves of some of the calculated half-order spots compared to that of the (1,0) spot.

It would appear that the 3×2 unit cell produces a 3×2 LEED pattern with half-order spots that are so weak in intensity that they fall below the background intensity, leaving only a 3×1 LEED pattern visible.

VII. DISCUSSION

The Pendry *R* factors obtained upon comparison of the *ab initio* calculations with experiment are not as low as we would expect. We can see that for some spots, the *I-V* curves are visually very similar to those obtained experimentally [see the *I-V* curves for the (1,1/3) and (2,0) spots, for example] but they have a poor *R* factor. This suggests that the structure is very nearly right and the minor discrepancy could be a result of our not including enough bulklike silicon layers in the bottom of the supercell with consequent effects on the reconstruction within the top honeycomb layer. We have attempted some simple variation in the top layer structure, for example, flattening the layer, but this drastically worsens the *R* factor. Computational resources prohibit us from calculating the structure with more silicon layers and from investigating the honeycomb layer structure further using LEED *I-V*. Perhaps further study with a LEED *I-V* genetic algorithmn search might optimize this structure further.

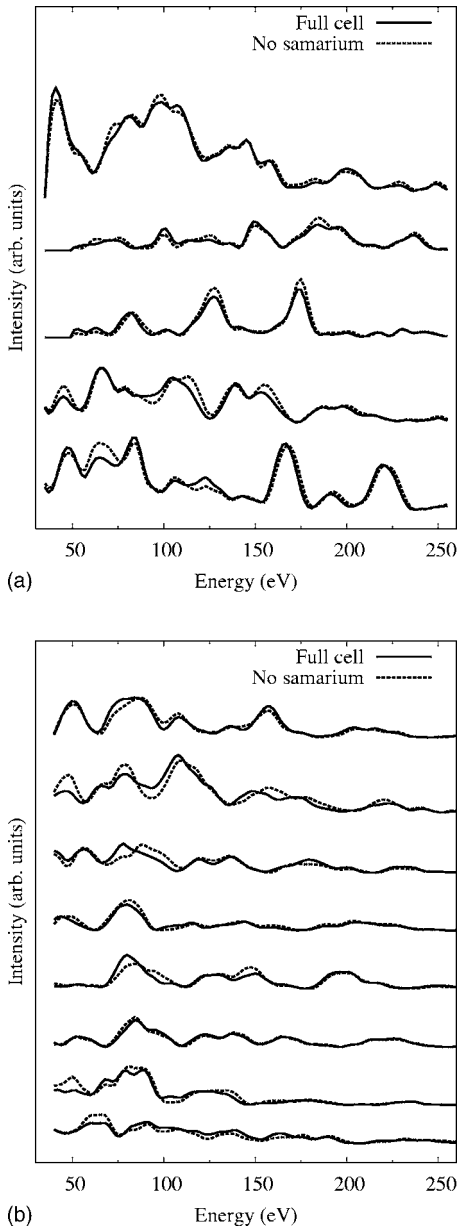

FIG. 12. Calculated LEED *I-V* curves for the integer spots (a) and fractional spots (b) of the H3 unit cell with and without the samarium atom in place. Bulk Debye temperatures were used throughout.

The moderate *R* factors are offset by the fact that two independent techniques both show optimum structural fits for almost identical interlayer spacings.

The lateral atomic structure was freely varied in the *ab initio* calculations in this work and the lateral atomic positions agree well with those found by Palmino *et al.*,[5] which they have shown to be in good qualitative agreement with experimental STM images. In this work, we have concentrated on the optimization of the vertical spacings, to which LEED is particularly sensitive.

The *R* factors for the integer spots are consistently worse than those for the fractional spots. There is the possibility that there are some regions in which there is a disordered overlayer of samarium atop a bulk terminated Si(111)-1×1

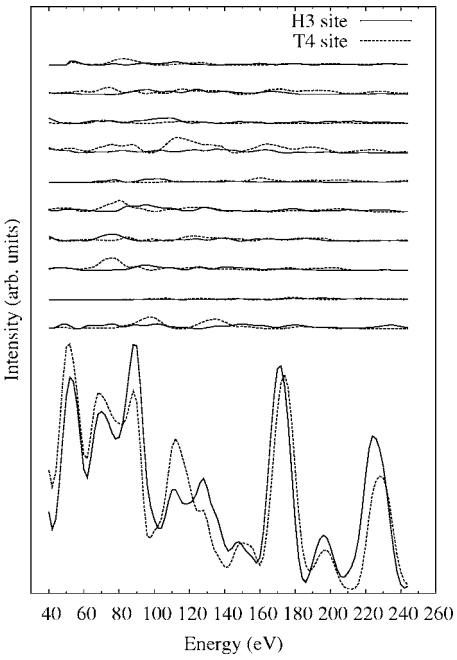

FIG. 13. Calculated *I-V* curves for the HCC structure showing the difference in the intensity (typically an order of magnitude) between the half-order spots and a representative spot that is visible in the LEED pattern during an experiment.

surface. Such a phase has been reported by Wigren *et al.*[26] The integer spots from such regions might contribute to the overall integer spots for the surface and reduce the level of agreement with the calculated *I-V* curves for the pure 3×2 surface.

We have not been able to determine the long-range order in the system. We might expect that simple electrostatic repulsion along the one-dimensional chain would space out the metal atoms and provide large separate domains of the H3 and the T4 structures. However, the two sites are almost degenerate and there would be an entropic gain from disorder. In the literature, one can find evidence for both order and disorder in the long-range positions of the metal atoms. In this study, the improvement in the Pendry *R* factor when the T4 and H3 structures are considered together on the surface suggests that both sites are occupied within the surface. We have also shown that we do not require more than one unit cell to explain the missing half-order spots in the LEED pattern and our experimentally observed LEED patterns show a low background due to good order on the surface. It could be that there is long-range disorder on the surface and that the coupling between many adjacent H3 and T4 unit cells and matching of the interlayer spacings introduce a slight strain that changes the structure in the honeycomb layer and the first bulklike layer enough to account for our Pendry *R* factors. If this is the case, then it would be impossible to obtain the structure of the honeycomb layer to a high degree of accuracy without an *ab initio* calculation using a supercell that comprises several thousand unit cells of the H3 and T4 structures randomly tesselated in both directions.

VIII. SUMMARY

We have provided a quantitative validation of the honeycomb chain channel model common to the 3×1 and 3×2 structures formed by alkali, alkali-earth, and rare-earth metals on Si(111). Several *I-V* data sets were obtained from LEED experiments and used to fingerprint the surface. The atomic structure suggested by our two *ab initio* calculations is in reasonable agreement with these experimental data. Further structural optimization and mapping of the *R* factor landscape have shown that a slight outward expansion of the top layer improves the fit somewhat, but increasing the vibrations in the top two layers gives a significant improvement. A linear combination of the two HCC structures has been shown to improve the fit still further, with the ratio being slightly in favor of the structure with the lower energy of the two. Finally, we have calculated the intensities of the half-order spots and shown that they are sufficiently dim to fall below the background intensity in a LEED experiment. Little change in the calculated *I-V* curves results from removing the samarium atom, which supports the idea that as a scattering unit the silicon honeycomb layer dominates the unit cell and makes LEED insensitive to the metal atom in these $3\times$ systems.

ACKNOWLEDGMENTS

Many thanks to F. Palmino for kindly providing the atomic coordinates for the Si(111)-3×2 unit cell. C.E. would like to acknowledge the EPSRC for financial support. This work made use of the facilities of HPCx, UK's national high-performance computing service, which is provided by EPCC at the University of Edinburgh and by CCLRC Daresbury Laboratory, and funded by the Office of Science and Technology through EPSRC's High End Computing Programme.

*Corresponding author. Email address: spt1@york.ac.uk

[1] A. A. Saranin, A. V. Zotov, S. V. Ryzhkov, D. A. Tsukanov, V. G. Lifshits, J.-T. Ryu, O. Kubo, H. Tani, T. Harada, M. Katayama, and K. Oura, Phys. Rev. B **58**, 7059 (1998).

[2] H. H. Weitering, X. Shi, and S. C. Erwin, Phys. Rev. B **54**, 10585 (1996).

[3] K. Sakamoto, W. Takeyama, H. M. Zhang, and R. I. G. Uhrberg, Phys. Rev. B **66**, 165319 (2002).

[4] G. Lee, S. Hong, H. Kim, D. Shin, J.-Y. Koo, H.-I. Lee, and Dae Won Moon, Phys. Rev. Lett. **87**, 056104 (2001).

[5] F. Palmino, E. Ehret, L. Mansour, J.-C. Labrune, G. Lee, H. Kim, and J.-M. Themlin, Phys. Rev. B **67**, 195413 (2003).

[6] M. Kuzmin, R.-L. Vaara, P. Laukkanen, R. Perälä, and I. J. Väyrynen, Surf. Sci. **538**, 124 (2003).

[7] H. H. Weitering, Surf. Sci. **355**, L271 (1996).

[8] D. Jeon, T. Hashizume, T. Sakurai, and R. F. Willis, Phys. Rev. Lett. **69**, 1419 (1992).

[9] C. Wigren, J. N. Andersen, R. Nyholm, M. Gothelid, M. Hammar,

C. Tornevik, and U. O. Karlsson, Phys. Rev. B **48**, 11014 (1993).
[10] J. Quinn and F. Jona, Surf. Sci. **249**, L307 (1991).
[11] W. C. Fan and A. Ignatiev, Phys. Rev. B **41**, 3592 (1990).
[12] C. Collazo-Davila, D. Grozea, and L. D. Marks, Phys. Rev. Lett. **80**, 1678 (1998).
[13] L. Lottermoser, E. Landemark, D.-M. Smilgies, M. Nielsen, R. Feidenhansl, G. Falkenberg, R. L. Johnson, M. Gierer, A. P. Seitsonen, H. Kleine, H. Bludau, H. Over, S. K. Kim, and F. Jona, Phys. Rev. Lett. **80**, 3980 (1998).
[14] S. C. Erwin and H. H. Weitering, Phys. Rev. Lett. **81**, 2296 (1998).
[15] J. Schäfer, S. C. Erwin, M. Hansmann, Z. Song, E. Rotenberg, S. D. Kevan, C. S. Hellberg, and K. Horn, Phys. Rev. B **67**, 085411 (2003).
[16] H. Over, M. Gierer, H. Bludau, G. Ertl, and S. Y. Tong, Surf. Sci. **314**, 243 (1994).
[17] V. E. de Carvalho, M. W. Cook, P. G. Cowell, O. S. Heavens, M. Prutton, and S. P. Tear, Vacuum **34**, 893 (1984).
[18] F. Palmino, E. Ehret, L. Mansour, E. Duverger, and J.-C. Labrune, Surf. Sci. **586**, 56 (2005).
[19] J. B. Pendry, J. Phys. C **13**, 937 (1980).
[20] M. D. Segall, P. J. D. Lindan, M. J. Probert, C. J. Pickard, P. J. Hasnip, S. J. Clark, and M. C. Payne, J. Phys.: Condens. Matter **14**, 2717 (2002).
[21] M. I. J. Probert and M. C. Payne, Phys. Rev. B **67**, 075204 (2003).
[22] H. J. Monkhorst and J. D. Pack, Phys. Rev. B **13**, 5188 (1976).
[23] J. P. Perdew, K. Burke, and M. Ernzerhof, Phys. Rev. Lett. **77**, 3865 (1996).
[24] D. J. Titterington and C. G. Kinniburgh, Comput. Phys. Commun. **20**, 237 (1980).
[25] H. Over, H. Huang, S. Y. Tong, W. C. Fan, and A. Ignatiev, Phys. Rev. B **48**, 15353 (1993).
[26] C. Wigren, J. N. Andersen, R. Nyholm, and U. O. Karlsson, Surf. Sci. **293**, 254 (1993).